Mitigating Cascading Failures via Local Responses

Chen Liang*, Fengyu Zhou*, Alessandro Zocca†, Steven H. Low* and Adam Wierman*
* Division of Engineering & Applied Science, California Institute of Technology, Pasadena, USA
† Department of Mathematics, Vrije Universiteit, Amsterdam, Netherlands
{cliang2, f.zhou, slow, adamw}@caltech.edu, a.zocca@vu.nl

***Abstract*—This work proposes an approach for failure mitigation in power systems via corrective control named Optimal Injection Adjustment (OIA). In contrast to classical approaches, which focus on minimizing load loss, OIA aims to minimize the post-contingency flow deviations by adjusting node power injections in response to failures. We prove that the optimal control actions obtained from OIA are localized around the original failure. Specifically, at any given node an injection adjustment is not required unless at least one of its neighboring nodes closer to the failure already reached its adjustment limit. Numerical simulations highlight that OIA achieves near-optimal control costs despite using localized control actions.**

I. Introduction

Reliability is a critical goal for power systems. Large-scale blackouts, although rare, cause significant economic and social impact. Typically, the start of a large-scale blackout is an initial individual failure that triggers a cascade of failures. To prevent such cascading failures, the power system is required to operate under certain security criteria: *preventive* security [1] criteria ensure that the power system remains safe after a contingency without any additional control actions, and *corrective* security [2] criteria provide post-contingency control actions that ensure the system remains stable.

As the power grid becomes increasingly stressed by more volatile demand fluctuations, improving the grid reliability is crucial. Additionally, the rapid growth of renewable penetration also poses challenges for grid reliability. Indeed, the increased and strongly correlated uncertainty from renewable energy sources makes preventive security less robust. To fully account for such uncertainty, power systems that operate under preventive security criteria are forced to have larger reserves and thus incur higher costs. On the other hand, technology advances with ubiquitous monitoring and control provide the possibility of implementing corrective actions in response to failures in real time [3].

Various corrective control policies have been proposed in the literature, such as transmission system reconfiguration and controlled system islanding, which involves line switching actions [4], [5], and generation rescheduling and load shedding, which encompass the adjustment of operational set-points [6]. In this paper, we focus on corrective controls using power injection adjustments, rather than topological approaches.

While existing corrective strategies exploit the flexibility of controllable devices in response to contingencies, the control actions for set-point adjustments are often designed using heuristics, e.g., uniformly scaling down the injections [7], which may result in a large amount of load loss. A variety of optimization-based corrective control policies have been proposed in [3], [8], [9], where the objective is to minimize the cost of control actions while ensuring that the post-contingency operating condition is safe. However, those optimizations are usually solved in a centralized manner and the structural properties of the solutions obtained are not well understood. It is thus difficult to consider applying these designs to large-scale networks, where fast and accurate control actions are required.

In this paper, we propose a different approach for corrective control that has strong structural properties. We refer to the proposed policy as *Optimal Injection Adjustment* (OIA). Our contribution is two-fold. We first theoretically prove that the control resulting from OIA exhibits a local injection adjustment pattern: at any given node an injection adjustment is not required unless at least one of its neighboring nodes closer to the contingency already reached its adjustment limit. Secondly, we compare OIA with traditional optimization-based corrective controls that focus on optimal load shedding (OLS) using numerical experiments. These experiments highlight that OIA achieves near-optimal control costs using localized control actions. Specifically, OIA requires 80% fewer nodes to adjust their operational set-points than traditional OLS, yet achieves similar control costs. However, to achieve local response, OIA sometimes pushes lines toward (or beyond) their capacity limit and so we additionally consider a variation, named OIA-LL, which imposes line limits explicitly in order to ensure that the adjustments prescribed by OIA-LL do not overload any lines. Our experiments highlight that OIA-LL provides nearly the same benefits as OIA with respect to control costs and that the injection adjustments, though less local than OIA, are still significantly more localized than that under OLS.

The design of OIA paves the way for further study of local corrective control policies. By exposing the topological pattern of optimal corrective actions, our analytic results show that it is possible to provide near-optimal corrective control using local injection adjustments. Such a structural property is highly desirable in large-scale power networks where distributed fast control policies are preferred. Further, our numerical results highlight the trade-off between the locality and control costs, especially when it comes to enforcing line capacity limits.

II. Model

This paper studies how to design an injection response that prevents a cascade following an initial contingency. To begin, in this section we introduce the DC power flow model and characterize how the flow redistribution happens after a failure.

A. DC Power Flow

We consider a power transmission network represented by a connected directed graph $\mathcal{G} = (\mathcal{V}, \mathcal{E})$, whose nodes $\mathcal{V} = \{1, 2, \dots, |\mathcal{V}|\}$ model network buses and edges $\mathcal{E} \subset \mathcal{V} \times \mathcal{V}$ model the transmission lines for which a fixed but arbitrary direction has been assigned. We use the terms bus/node and line/edge interchangeably and denote the line $l \in \mathcal{E}$ connecting nodes i and j also as (i, j).

We adopt the widely used (linearized) DC power flow model as an approximation for the non-linear and non-convex AC power flow model in which the transmission lines are modeled as purely reactive. Each line $l = (i, j)$ is characterized by its susceptance $b_l = b_{ij} > 0$ and we define the susceptance matrix as $B = \operatorname{diag}(b_l, l \in \mathcal{E}) \in \mathbb{R}^{|\mathcal{E}|\times|\mathcal{E}|}$. The network topology is captured by the node-edge incidence matrix $C \in \mathbb{R}^{|\mathcal{V}|\times|\mathcal{E}|}$ defined as follows: for every line $l = (i, j)$, $C_{il} = 1$, $C_{jl} = -1$, and we set to zero all other entries in the column corresponding to that line. The graph Laplacian is the matrix $L = CBC^T$ and we denote its pseudoinverse as $L^\dagger$.

Given the power injections and phase angles $\boldsymbol{p}, \boldsymbol{\theta} \in \mathbb{R}^{|\mathcal{V}|}$, the branch flows $\boldsymbol{f} \in \mathbb{R}^{|\mathcal{E}|}$ are obtained as the solution to the following *DC power flow equations*:

$$\boldsymbol{p} = C\boldsymbol{f}, \tag{1a}$$

$$\boldsymbol{f} = BC^T\boldsymbol{\theta}. \tag{1b}$$

It is known that there exists a unique branch flow solution $\boldsymbol{f} = BC^T L^\dagger \boldsymbol{p}$ to the above power flow equations, provided that the power injections are balanced ($\sum_{j\in\mathcal{G}} p_j = 0$) for the graph $\mathcal{G}$ [10] . Using a classical result in circuit analysis [11], it is easy to show that the branch flow solution of (1) is also the unique optimal solution of the following quadratic optimization problem:

$$\min_{\boldsymbol{f}} \quad \boldsymbol{f}^T B^{-1} \boldsymbol{f} \tag{2a}$$

$$\text{s.t.} \quad \boldsymbol{p} = C\boldsymbol{f}. \tag{2b}$$

The quadratic form $\boldsymbol{f}^T B^{-1} \boldsymbol{f} = \sum_{l\in\mathcal{E}} b_l^{-1} f_l^2$ that appears as the objective function has been shown in [12] to be an approximation for the power losses in the AC network. The same quantity has also been studied in [13] and [14], where it is referred to as *network tension* and is proven to be monotonically increasing during any cascading failure process. In [13] it has been shown that while an arbitrary load shedding may increase the network tension, there exists a load shedding configuration that can guarantee its reduction.

B. Power Redistribution After a Failure

Our goal is to understand how to respond to a failure. For the sake of simplicity, we consider a single-line outage that leaves the post-contingency network connected. Our results can be extended to multiple line outages at the expense of complexity of presentation.

The approach we use relies on the spectral representation developed in [14]. To distinguish between pre- and post-contingency quantities, we add a superscript $(\cdot)^{\text{pre}}$ to those referring to pre-contingency network. Specifically, we assume the pre-contingency network $\mathcal{G}^{\text{pre}} = (\mathcal{V}^{\text{pre}}, \mathcal{E}^{\text{pre}})$ comprises the same nodes, i.e., $\mathcal{V}^{\text{pre}} = \mathcal{V}$, and has exactly one more transmission line, namely $\mathcal{E}^{\text{pre}} = \mathcal{E} \cup \{e\}$, i.e., line $e = (s, t)$ is outaged. We denote its pre-contingency flow as $\alpha := f_e^{\text{pre}} = f_{s,t}^{\text{pre}} \in \mathbb{R}$. Denote by $\boldsymbol{f}_{-e} := (f_l, l \in \mathcal{E} \setminus \{e\}) \in \mathbb{R}^{|\mathcal{E}|}$ the vector of branch flows on the surviving lines. The post-contingency deviations of $\Delta\boldsymbol{p} = \boldsymbol{p} - \boldsymbol{p}^{\text{pre}}$, $\Delta\boldsymbol{\theta} = \boldsymbol{\theta} - \boldsymbol{\theta}^{\text{pre}}$ and $\Delta\boldsymbol{f} = \boldsymbol{f}_{-e} - \boldsymbol{f}_{-e}^{\text{pre}}$ satisfy:

$$\alpha\boldsymbol{e}_{s,t} + \Delta\boldsymbol{p} = C\Delta\boldsymbol{f}, \tag{3a}$$

$$\Delta\boldsymbol{f} = BC^T\Delta\boldsymbol{\theta}. \tag{3b}$$

Equation (3) suggests that the system deviations can be equivalently modeled by the DC power flow equations over the post-contingency network with injections $\alpha\boldsymbol{e}_{s,t} + \Delta\boldsymbol{p}$. The first term $\alpha\boldsymbol{e}_{s,t}$ characterizes the internal effect of redistributing the flow of the outaged line e. The second term $\Delta\boldsymbol{p}$ characterizes the external effect of injection adjustments of either generations or loads after the failure. Note that the power balancing condition $\sum_i \Delta p_i = 0$ is implicitly required to satisfy (3a).

III. Optimal Injection Adjustment

Given the model introduced in the previous section, we can now discuss how to respond to the initial failure. Here, we formulate an optimization problem that aims to minimize the flow deviations by adjusting the node power injections in response to line failures. The key to our approach is to focus on the post-contingency injection adjustments $\Delta\boldsymbol{p}$, which capture both generators and loads flexibility and are thus bounded by generator capacity limits or load shedding allowance. For any node $i \in \mathcal{V}$ we denote its injection adjustment and corresponding constraints as

$$\Delta\underline{p}_i \le \Delta p_i \le \Delta\overline{p}_i.$$

For each injection adjustment $\Delta\boldsymbol{p}$ satisfying the above constraints, the post-contingency flow deviations $\Delta\boldsymbol{f}$ can then be computed from (3).

We henceforth drop the notation $\Delta(\cdot)$ for compactness, but all the quantities $\boldsymbol{p}$, $\boldsymbol{f}$, and $\boldsymbol{\theta}$ will still denote *deviations* from their original values in the pre-contingency network.

We quantify the magnitude of the flow deviation on each surviving line l by means of a non-negative "cost function" $c_l(f_l)$, which we take to be strictly monotonically increasing with the absolute value of f_l. Given such a family of cost functions, we formulate the **optimal injection adjustment (OIA) problem**, whose goal is to determine the injection adjustments that minimize the cost of post-contingency flow deviations. Formally, given a pre-contingency network $\mathcal{G}^{\text{pre}}$ with a branch flow α on the line $e = (s, t) \in \mathcal{E}^{\text{pre}}$ to be tripped, the OIA(α,s,t) problem is formulated on the post-contingency network $\mathcal{G}$ as follows:

$$\min_{\boldsymbol{f},\boldsymbol{p},\boldsymbol{\theta}} \quad \sum_{l\in\mathcal{E}} c_l(f_l) \tag{4a}$$

$$\text{s.t.} \quad \alpha\boldsymbol{e}_{s,t} + \boldsymbol{p} = C\boldsymbol{f}, \tag{4b}$$

$$\boldsymbol{f} = BC^T\boldsymbol{\theta} \tag{4c}$$

$$\underline{\boldsymbol{p}} \le \boldsymbol{p} \le \overline{\boldsymbol{p}}. \tag{4d}$$

We assume that the generators and loads in our model are controllable and both components can either increase or decrease their injections. As a result, for every node $i \in \mathcal{V}$, its adjustment limit satisfies $\underline{p}_i < 0 < \overline{p}_i$.

To build intuition for the OIA problem, notice that ignoring the constraint (4d) yields a trivial (unique) optimal solution $\boldsymbol{p}^* = -\alpha \boldsymbol{e}_{s,t}$. This suggests that if the adjustments at the end-points of the failed transmission line are allowed to be large enough, i.e. $\max(\underline{p}_t, -\overline{p}_s) \leq \alpha \leq \min(\overline{p}_t, -\underline{p}_s)$, pre-contingency branch flows of the grid can be restored.

Beyond this simple case, the OIA problem can prioritize different system requirements by choosing appropriate cost functions. For instance, $c_l(f_l) = |f_l|$ characterizes the total post-contingency absolute flow deviations, which can be useful to determine the capacity reserves for transmission lines. Another possible cost function is $c_l(f_l) = b_l^{-1} f_l^2$. Note that f_l here indicates the flow deviation rather than the actual value used in network tension. This quantity has been studied in contingency analysis to quantify the severity of a line failure [15]. It is shown that the average load loss and number of outaged lines increase as this quantity increases. Thus, adjusting post-contingency injections to minimize this cost function can potentially improve grid stability against failures.

While not immediately clear, the OIA problem ensures a local response to contingencies. In particular, we show in the next section that the optimal solutions of the OIA problem exhibit a local and progressive pattern. Specifically, the optimal adjustments are localized around the failure in a way that an injection adjustment is non-zero only if at least one of its neighbors reaches the adjustment limit. This topological pattern in the adjustments ensures that it is possible to design local responses against failures while avoiding computational challenges. This is particularly important when the system requires fast timescale post-contingency corrective control policies for reliability.

A drawback of the OIA problem introduced so far is that it does not explicitly constrain post-contingency flows to satisfy the line capacity limits. As a result there may be some lines that are overloaded post-contingency. When this is a problem, it can be remedied by including the constraints explicitly via

$$\underline{\boldsymbol{f}} \leq \boldsymbol{f} \leq \overline{\boldsymbol{f}}, \tag{5}$$

where $\underline{\boldsymbol{f}}$ and $\overline{\boldsymbol{f}}$ are the limits for post-contingency flow deviations. We refer to the OIA with above line limits as the **optimal injection adjustment with line limits (OIA-LL) problem**. While our analytic results focus on OIA, we show via case studies in Section V that OIA-LL achieves nearly the same performance as OIA at the expense of some locality.

Finally, note that the OIA problem we consider is philosophically different than traditional corrective control policies, e.g., see [9], [16]. In these works, the focus is on the **optimal load shedding (OLS) problem** whose objective is to minimize the cost of load loss. Formally, a generalization of OLS can be formulated as:

$$\begin{aligned} \min_{\boldsymbol{f},\boldsymbol{p},\boldsymbol{\theta}} \quad & \sum_{i \in \mathcal{V}} c_i(p_i) && \text{(6a)}\\ \text{s.t.} \quad & \alpha \boldsymbol{e}_{s,t} + \boldsymbol{p} = C\boldsymbol{f}, && \text{(6b)}\\ & \boldsymbol{f} = BC^T\boldsymbol{\theta} && \text{(6c)}\\ & \underline{\boldsymbol{p}} \leq \boldsymbol{p} \leq \overline{\boldsymbol{p}}, && \text{(6d)}\\ & \underline{\boldsymbol{f}} \leq \boldsymbol{f} \leq \overline{\boldsymbol{f}}, && \text{(6e)} \end{aligned}$$

where the objective is to explicitly minimize the cost of injection adjustments $c_i(p_i)$ (e.g. the loss of load, the cost of generator ramping) while enforcing post-contingency flows under line capacity as a constraint (6e). This is a generalization of classical OLS because it allows loads to fluctuate both up and down around the pre-contingency injection, instead of only down. This generalization allows for a more fair comparison between OLS and OIA.

In contrast to OLS, the OIA problem does not minimize the cost of injection adjustments directly, but encodes the adjustment limit into constraint (4d). Specifically, the traditional approaches tend to impose a larger adjustment limit in (6d) in order to make the optimization feasible. On the other hand, the OIA problem (4) is always feasible and one can impose a more strict limit in (4d) so that a lower cost for control actions is implicitly achieved. It should be noted, however, that a strict injection adjustment limit may result in unsafe post-contingency line flows. Therefore, the limit should be designed carefully based on the system parameters and application scenarios. As we will show in Section V through numerical experiments, the OIA provides a near-optimal but much more local injection adjustments in response to failures. The overloaded lines are avoided with the OIA-LL method.

IV. Analysis

The remainder of this paper studies the OIA and OIA-LL problems and their benefits for contingency response. In this section, we provide analytic results that characterize the topological patterns of the optimal solutions to the OIA problem. These patterns lead to possible local, distributed and fast responses against failures.

We begin with the case where the post-contingency network is a tree. In this case, for any choice of the cost functions, the optimal solutions of the OIA problem have a distinctive feature: the injection of any node is not adjusted unless its preceding nodes toward the endpoints s and t of the outaged line reach their adjustment limits. We prove that a similar characterization holds for general post-contingency networks (possibly including loops) if the cost function $c_l(f_l) = b_l^{-1} f_l^2$ is used. Recall that this cost prioritizes grid stability.

For ease of presentation, we assume the direction of pre-contingency flow over the outage line $e = (s, t)$ is from node s toward node t, i.e. $\alpha > 0$. All proofs in this section are deferred to Appendix.

A. Tree Post-Contingency Network

We first analyze the optimal solutions of the OIA problem (4) in the case in which the post-contingency network $\mathcal{G}$

is a tree. Our main result, Theorem 3, states that the optimal injection adjustment at each node i can be determined by checking whether the adjustment limit is reached by all the *preceding* nodes (see Definition 1) along the paths connecting node i toward nodes s and t.

Definition 1. *Given two nodes i, j, consider a simple path (i.e., without repeated nodes) $P = [i = u_0, u_1, u_2, \ldots, u_r = j]$ connecting nodes i and j. We denote the node preceding node j in the path P toward node i as $u_i^P(j) := u_{r-1}$, and denote the set of all nodes preceding node j along the path P as $\mathcal{U}_i^P(j) := \{i = u_0, u_1, \ldots, u_{r-1}\}$. Moreover, we define $\mathcal{U}_i^P(i) = \emptyset$.*

Note that there exists a unique simple path for every pair of nodes i and j when the post-contingency network is a tree. Thus we omit the superscript $(\cdot)^P$ in this subsection for notation simplicity.

In order to build to the presentation of Theorem 3, we develop a construction of the post-contingency flow deviations $\boldsymbol{f} \in \mathbb{R}^{|\mathcal{E}|}$. In general, the power flow equation (1b) requires $\boldsymbol{f}$ to lie in the column space of matrix BC^T; however, such an image space is essentially $\mathbb{R}^{|\mathcal{E}|}$ as $\mathrm{range}(BC^T) = |\mathcal{E}|$ when the post-contingency network is a tree [17]. Therefore, constraint (4c) in OIA problem is actually redundant for tree networks, since for any arbitrary flow vector $\boldsymbol{f} \in \mathbb{R}^{|\mathcal{E}|}$, we can always construct the corresponding phase angles $\boldsymbol{\theta}$ and power injections $\boldsymbol{p}$ such that the DC power flow equations (4c) and (4b) naturally hold. In particular, we have $\boldsymbol{\theta} = L^\dagger C \boldsymbol{f}$ and $\boldsymbol{p} = C\boldsymbol{f} - \alpha \boldsymbol{e}_{s,t}$.

This fact plays a critical role in the proof of the following lemma, which characterizes the necessary conditions to determine the sign of optimal injection adjustment for every node i other than nodes s or t.

Lemma 2. *Assume that the cost function is strictly increasing in absolute flow deviations and that the post-contingency network is a tree. For node $i \neq s, t$ and its preceding node $u_s(i)$ toward node s and preceding node $u_t(i)$ toward node t, the optimal solutions $\boldsymbol{p}^*, \boldsymbol{f}^*$ of the optimization (4) satisfy:*

- *If $p_i^* > 0$, then $f^*_{u_t(i),i} < 0$, $p^*_{u_t(i)} = \overline{p}_{u_t(i)}$;*
- *If $p_i^* < 0$, then $f^*_{u_s(i),i} > 0$, $p^*_{u_s(i)} = \underline{p}_{u_s(i)}$.*

Lemma 2 suggests that for any given node i other than nodes s or t, if the optimal control is to increase its injection, then its preceding node $u_t(i)$ toward node t must reach the maximal adjustment limit. Moreover, the direction of corresponding optimal flow deviation is from node i toward node $u_t(i)$. Similarly, if the optimal control at node i is to decrease its injection, then the preceding node $u_s(i)$ toward node s reaches the minimal adjustment limit with the flow deviation from node $u_s(i)$ toward node i.

Applying Lemma 2 repeatedly, one can show that if the optimal injection adjustment at node i is non-zero, then there must exist a path connecting node i to node s or t along which the optimal injection adjustments of all the nodes reach their limits. Moreover, the direction of optimal flow deviations are determined based on the sign of p_i^*. We formally characterize this topological pattern in the following theorem, which is the main result of this section.

Theorem 3. *Assume the post-contingency network is a tree and that the cost function is strictly increasing in absolute flow deviations. For any optimal solutions $\boldsymbol{p}^*$ of (4), the optimal injection adjustment at node $i \neq s, t$ satisfies:*

(a) *If there exists $j \in \mathcal{U}_t(i)$ with $p_j^* < \overline{p}_j$, then $p_i^* \leq 0$;*
(b) *If there exists $j \in \mathcal{U}_s(i)$ with $p_j^* > \underline{p}_j$, then $p_i^* \geq 0$.*

In particular, if there exist both $j \in \mathcal{U}_t(i)$ with $p_j^* < \overline{p}_j$ and $j' \in \mathcal{U}_s(i)$ with $p_{j'}^* > \underline{p}_{j'}$, then $p_i^* = 0$.

Theorem 3 illustrates that the optimal solution to (4) is to progressively adjust the injections starting from nodes s and t, which aligns with intuition. Specifically, the contingency causes an excessive injection α at node s and a power deficit $-\alpha$ at node t for the post-contingency system. To compensate for such imbalances, the optimal response at every other node depends on its preceding nodes toward the endpoints of the failures. In particular, there is no incentive for a node to adjust its injection when there is a preceding node that does not reach its adjustment limit. Therefore, the injection adjustments follow a progressive pattern from the endpoints of the contingency. In fact, there is an (tight) upper bound for the total absolute injection adjustments of all the nodes as shown in the following lemma.

Lemma 4. *Assume the post-contingency network is a tree and that the cost function is strictly increasing in absolute flow deviations. Then, every optimal solutions $\boldsymbol{p}^*$ of (4) satisfies the following inequalities: (i) $p_s^* < 0$ and $p_t^* > 0$; (ii) $\sum_{i \in \mathcal{V}} |p_i^*| \leq 2\alpha$.*

The next corollary follows immediately from combining Theorem 3 and Lemma 4. It suggests that the progressive injection adjustments are guaranteed to terminate so that the adjusted nodes are localized around nodes s and t.

Corollary 5. *Assume the post-contingency network is a tree and that the cost function is strictly increasing in absolute flow deviations. Then, for any optimal solutions $\boldsymbol{p}^*$ of (4) the optimal injection adjustment p_i^* at node $i \neq s, t$ satisfies the following properties:*

- *If $\sum_{j \in \mathcal{U}_s(i)} -\underline{p}_j \geq \alpha$, then $p_i^* \geq 0$;*
- *If $\sum_{j \in \mathcal{U}_t(i)} \overline{p}_j \geq \alpha$, then $p_i^* \leq 0$.*

In particular, if both $\sum_{j \in \mathcal{U}_s(i)} -\underline{p}_j \geq \alpha$ and $\sum_{j \in \mathcal{U}_t(i)} \overline{p}_j \geq \alpha$ hold, then $p_i^* = 0$.

B. General Post-Contingency Networks

The characterization proved in the case of tree networks does not hold in general. However, we show here that the localization properties observed in the case of tree networks extend to general networks when the cost function $c_l(f_l) = b_l^{-1} f_l^2$ is adopted. Recall that the cost function $c(\boldsymbol{f}) = \boldsymbol{f}^T B^{-1} \boldsymbol{f}$ is popular in the contingency literature, where it is usually regarded as a metric to quantify the severity of a failure.

Loops complicate the behavior of general networks as there may be multiple simple paths connecting nodes i and j.

For clarity, in this subsection we add back the superscript $(\cdot)^P$ for $u_i^P(j)$ and $\mathcal{U}_i^P(j)$ to indicate a specific simple path P connecting node j towards node i. We now present the main result of this section, which extends Theorem 3 to general networks and characterizes the conditions to determine post-contingency injection deviations. Moreover, if the post-contingency injections for both endpoints of a transmission line remain the same, the post-contingency flow is unchanged as well, suggesting that flow deviations are localized along the lines with adjusted injections.

Theorem 6. *Assuming a connected post-contingecny network and taking* $c_l(f_l) = b_l^{-1} f_l^2$ *as cost function, the optimal injection adjustment* p_i^* *at node* $i \neq s, t$ *for the optimal solution* $\boldsymbol{p}^*$ *of* (4) *satisfies the following properties:*

- (a) *If for every simple path* P *connecting node* i *and* t *there exists* $j \in \mathcal{U}_t^P(i)$ *with* $p_j^* < \overline{p}_j$*, then* $p_i^* \leq 0$*;*
- (b) *If for every the simple path* P *connecting node* i *and* s *there exists* $j \in \mathcal{U}_s^P(i)$ *with* $p_j^* > \underline{p}_j$*, then* $p_i^* \geq 0$*.*

In addition, for line $(i, j) \in \mathcal{E}$*, if* $\underline{p}_i < p_i^* < \overline{p}_i$ *and* $\underline{p}_j < p_j^* < \overline{p}_j$*, then we have* $f_{i,j}^* = 0$*.*

Similarly to Corollary 5 in the case of a tree post-contingency network, the optimal injection adjustments are localized around the endpoints of the failure for general networks as well. We formalize this in the following result.

Corollary 7. *Assuming a connected post-contingecny network and taking* $c_l(f_l) = b_l^{-1} f_l^2$ *as cost function, the optimal injection adjustment at any node* $i \neq s, t$ *for the optimal solution* $\boldsymbol{p}^*$ *of* (4) *satisfies the following properties:*

- *If* $\sum_{j \in \mathcal{U}_s^P(i)} -\underline{p}_j \geq \alpha$ *for all simple paths* P *connecting node* i *toward node* s*, then* $p_i^* \geq 0$*;*
- *If* $\sum_{j \in \mathcal{U}_t^P(i)} \overline{p}_j \geq \alpha$ *for all simple paths* P *connecting node* i *toward node* t*, then* $p_i^* \leq 0$*.*

An implicit, but important, component of the above results is that the optimal injection adjustments are localized around the line failure, which provides computational gains. Specifically, define the following quantities for every node $i \neq s, t$:

$$d_s(i) = \min_P \sum_{j \in \mathcal{U}_s^P(i)} -\underline{p}_j \quad \text{and} \quad d_t(i) = \min_P \sum_{j \in \mathcal{U}_t^P(i)} \overline{p}_j.$$

These two quantities can be computed for every node in the network using a variant of Dijkstra's algorithm with complexity $\mathcal{O}(n^2)$. Corollary 7 suggests that for a single line failure (s, t), the optimal injection adjustments will be localized within a subset of nodes around node s and t of α, i.e., for node $i \in \mathcal{V}_{st}(\alpha) := \{v \in \mathcal{V} : d_s(v) \geq \alpha, d_t(v) \geq \alpha\}$, $p_i^* = 0$. Moreover, for a line (i, j) with $i, j \in \mathcal{V}_{st}(\alpha)$, $f_{i,j}^* = 0$. This localized pattern helps accelerate the computation of (4). For instance, the size of set $\mathcal{V} \backslash \mathcal{V}_{st}(\alpha)$ is usually much smaller than the actual network size. Many variables in (4) can thus be set as 0 and redundant constraints can be removed, allowing for a faster and more local response against failures.

V. Case Study

In this section, we use numerical simulations to evaluate the performance of OIA and OIA-LL in response to failures in the IEEE 118-bus test network and compare it with a classical corrective control approach, OLS.

A. Setup

We simulate failure scenarios for the IEEE 118-bus test network, using the system parameters and the pre-contingency operating conditions described in [18]. We associate each transmission line with a capacity that is 1.2 times the amount of pre-contingency flow on that line. Considering individually every transmission line whose removal does not disconnect the network as the initial failure, we simulate the post-contingency system state under three control policies (OIA, OIA-LL, and OLS) and additionally contrast these with what happens when no control is applied.

For OIA, we select $c_l(f_l) = b_l^{-1} f_l^2$ as the cost function since the post-contingency network is not a tree in general. For every node i we set the adjustment limits proportionally to its pre-contingency injection, namely

$$-\beta \, |p_i^{\text{pre}}| \leq p_i \leq \beta \, |p_i^{\text{pre}}| \, ,$$

with $\beta > 0$. In our simulations we choose $\beta = 0.1, 0.3, 1.0$ to represent various levels of the injection adjustment limit, where a larger β captures a more lenient allowance. For its variation OIA-LL that enforces line limits as well, we choose $\beta = 1.0$ to guarantee its feasibility.

For the traditional corrective control OLS, recall that we allow generations and loads to fluctuate around the pre-contingency values for a fair comparison with OIA. We thus use $c_i(p_i) = |p_i|$ as the cost function to penalize the total post-contingency injection adjustments. Similarly to OIA-LL, we choose $\beta = 1.0$ so that OLS is guaranteed to be feasible.

B. The performance of OIA

To illustrate the performance of OIA, we study the trade-off between locality and injection adjustment as a function of the post-contingency injection adjustment flexibility, captured by the parameter β.

Figure 1 illustrates the failure mitigation performance of OIA for different β's. Specifically, we investigate the fraction of transmission lines whose post-contingency flows exceed line capacity and the relative injection adjustment to the pre-contingency injections for every single-line failure. Figure 1 demonstrates the complementary cumulative distribution function (CCDF) for these two metrics. It is shown that, even under a strict adjustment limit (small β), OIA outperforms the baseline where no control is implemented in terms of preventing overloaded lines. Moreover, transmission lines become less likely to be overloaded as β increases. However, a more lenient limit potentially leads to larger injection adjustments.

Figure 2 compares the localization performance for OIA with various β's. To quantify the locality, we compute the fraction of nodes with adjusted injections and the radius (in hops) for the subset of adjusted nodes to the endpoints of

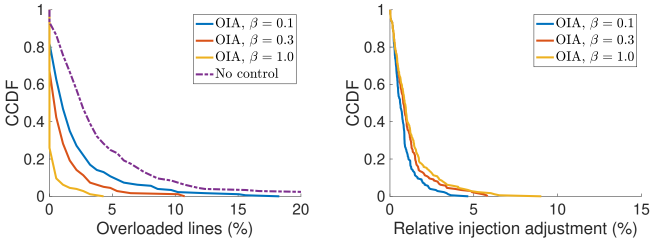

Figure 1. CCDF of the fraction of overloaded transmission lines (left) and the relative injection adjustment (right).

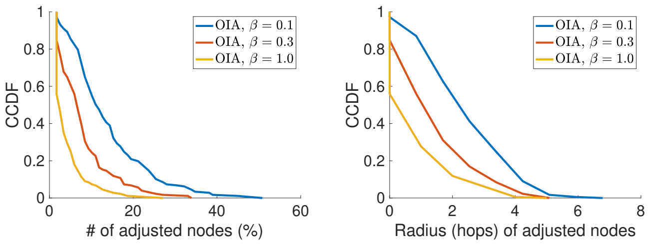

Figure 2. CCDF of the fraction of nodes with injection adjustment and the radius (in hops) of the adjusted nodes to the endpoints of an initial failure.

initial failure. Clearly, a larger β achieves better localization performance: fewer nodes that are closer to the contingency are adjusted for failure mitigation.

To summarize, a larger β prevents lines being overloaded and uses a more local response, at a possible cost of larger amount of injection adjustments. It is thus crucial to carefully tune the parameter β to prioritize different control objectives.

C. Comparing OIA and OLS

We now compare the performance of OIA and OIA-LL with the more traditional approach OLS. For a fair comparison, we fix $\beta = 1.0$ for OIA, to minimize the chance of overloaded lines. This results in fewer than 0.3% of lines being overloaded with OIA on average. We also compare OIA with its augmented version, OIA-LL, that directly enforces post-contingency line flows and hence has no overloaded lines.

Figure 3 illustrates the comparison between OIA, OIA-LL and OLS. Both OIA and OIA-LL achieve similar results in terms of the relative injection adjustments and the fraction of nodes with injection adjustment, while OIA-LL requires nodes from a broader region to participate in the mitigation process. Furthermore, OIA-LL leads to a larger portion of lines with flow deviations than OIA. On the other hand, OLS achieves smallest injection adjustments, but leads to largest amount of nodes and transmission lines affected after failures.

Figure 4 shows the Pareto curve for OIA, demonstrating the trade-off between the adjustment cost and the locality of control actions. The curve is generated by simulating with $\beta > 0.3$ for OIA so that the average number of overloaded lines remains below 1%. For comparison, we demonstrate the performance of OIA-LL and OLS as well. The key point here is that OLS is far from the Pareto frontier of OIA, thus highlighting that OIA achieves a better trade-off between localizing responses and the size of injection adjustments.

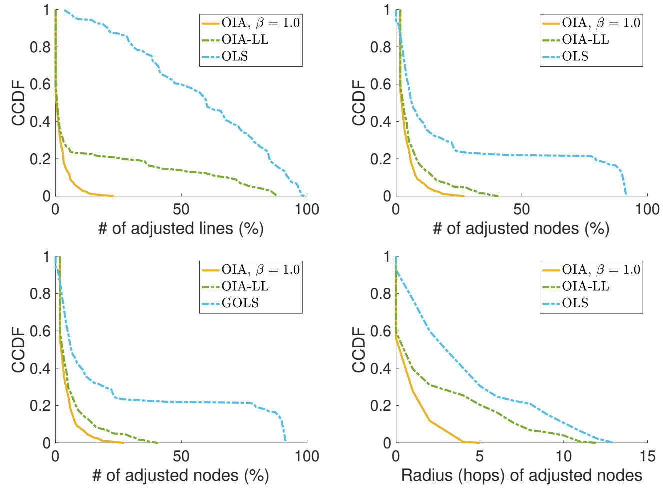

Figure 3. Comparison of OIA, OIA-LL and OLS.

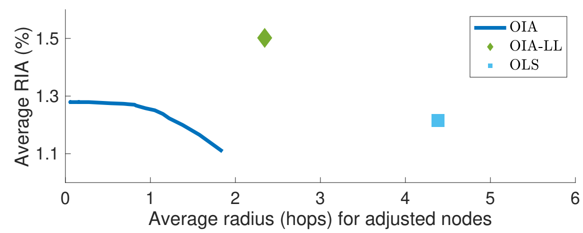

Figure 4. Pareto curve of OIA, OIA-LL, and OLS trading off relative injection adjustment (y-axis) and radius of adjusted nodes.

Enforcing line limits in OIA-LL means that it is also outside the Pareto frontier of OIA, but control still remains local, at the expense of a slightly larger control cost (note the scale of the y-axis); which means that it is closer to the Pareto frontier of OIA than OLS.

VI. Conclusions

In this paper, we have formulated a novel corrective control policy that achieves near-optimal control costs using localized control actions in response to failures. Both theoretical analysis and case studies validate the properties and capabilities of the proposed approach. This shows the feasibility of local corrective control, and there are a number of important directions for future exploration of this topic, e.g., (i) theoretical analysis for the trade-off between the locality and control costs, (ii) localized, distributed, and fast control policy design for large-scale power networks, (iii) analytical comparisons between the optimal injection adjustment and other corrective control policies, and (iv) generalization and validation with the non-linear AC power flow model.

References

[1] O. Alsac and B. Stott, “Optimal load flow with steady-state security,” *IEEE transactions on power apparatus and systems*, no. 3, pp. 745–751, 1974.

[2] A. Monticelli, M. Pereira, and S. Granville, “Security-constrained optimal power flow with post-contingency corrective rescheduling,” *IEEE Transactions on Power Systems*, vol. 2, no. 1, pp. 175–180, 1987.

[3] L. Roald, S. Misra, T. Krause, and G. Andersson, "Corrective control to handle forecast uncertainty: A chance constrained optimal power flow," *IEEE Transactions on Power Systems*, vol. 32, no. 2, pp. 1626–1637, 2016.
[4] X. Wang, W. Shao, and V. Vittal, "Adaptive corrective control strategies for preventing power system blackouts," *Proc. of 15th PSCC*, 2005.
[5] W. Shao and V. Vittal, "Corrective switching algorithm for relieving overloads and voltage violations," *IEEE Transactions on Power Systems*, vol. 20, no. 4, pp. 1877–1885, 2005.
[6] T. Medicherla, R. Billinton, and M. Sachdev, "Generation rescheduling and load shedding to alleviate line overloads-analysis," *IEEE Transactions on Power Apparatus and Systems*, no. 6, pp. 1876–1884, 1979.
[7] A. Bernstein, D. Bienstock, D. Hay, M. Uzunoglu, and G. Zussman, "Power grid vulnerability to geographically correlated failures 2014: analysis and control implications," in *IEEE INFOCOM*, April 2014, pp. 2634–2642.
[8] S. Koch, S. Chatzivasileiadis, M. Vrakopoulou, and G. Andersson, "Mitigation of cascading failures by real-time controlled islanding and graceful load shedding," in *2010 IREP Symposium Bulk Power System Dynamics and Control*. IEEE, 2010, pp. 1–19.
[9] M. Parandehgheibi, E. Modiano, and D. Hay, "Mitigating cascading failures in interdependent power grids and communication networks," in *Proc. of 2014 SmartGridComm*. IEEE, 2014, pp. 242–247.
[10] D. Bienstock and A. Verma, "The $n-k$ problem in power grids: New models, formulations, and numerical experiments," *SIAM Journal on Optimization*, vol. 20, no. 5, pp. 2352–2380, 2010.
[11] C. A. Desoer, *Basic circuit theory*. Tata McGraw-Hill Education, 2010.
[12] J. K. Johnson and M. Chertkov, "A majorization-minimization approach to design of power transmission networks," in *49th IEEE Conference on Decision and Control (CDC)*. IEEE, 2010, pp. 3996–4003.
[13] C. Lai and S. H. Low, "The redistribution of power flow in cascading failures," in *51st Annual Allerton Conference*, Oct 2013, pp. 1037–1044.
[14] L. Guo, C. Liang, and S. H. Low, "Monotonicity properties and spectral characterization of power redistribution in cascading failures," in *55th Annual Allerton Conference on Communication, Control, and Computing*, Oct 2017, pp. 918–925.
[15] S. Soltan, A. Loh, and G. Zussman, "Analyzing and quantifying the effect of k-line failures in power grids," *IEEE Transactions on Control of Network Systems*, vol. 5, no. 3, pp. 1424–1433, 2017.
[16] S. Pahwa, C. Scoglio, S. Das, and N. Schulz, "Load-shedding strategies for preventing cascading failures in power grid," *Electric Power Components and Systems*, vol. 41, no. 9, pp. 879–895, 2013.
[17] N. L. Biggs, *Algebraic graph theory*. Cambridge university press, 1993, vol. 67.
[18] R. D. Zimmerman, C. E. Murillo-Sánchez, and R. J. Thomas, "Matpower: Steady-state operations, planning, and analysis tools for power systems research and education," *IEEE Transactions on Power Systems*, vol. 26, no. 1, pp. 12–19, 2010.

APPENDIX

Proof of Lemma 2. We prove only the first claim as the proof of the second is analogous. Define $\hat{\boldsymbol{p}} := \boldsymbol{p}^* + \alpha \boldsymbol{e}_{s,t}$ which satisfies the flow conservation rule $\hat{\boldsymbol{p}} = C\boldsymbol{f}^*$. For sake of contradiction, assume $f^*_{u_t(i),i} \geq 0$. Since $\hat{p}_i = p^*_i > 0$ and $f^*_{u_t(i),i} \geq 0$, there must exist a node $v_1 \neq t$ with $f^*_{i,v_1} > 0$ due to the flow conservation rule. If $\hat{p}_{v_1} \geq 0$, we can further find another node $v_2 \neq t$ with flow directing from v_1 to v_2. Such a construction can be repeated until $\hat{p}_{v_k} < 0$ at node v_k. We remark that node v_k always exists, otherwise the flow conservation rule cannot be satisfied. In addition, $p^*_{v_k} < 0$ since $v_k \neq t$ and $\hat{p}_{v_k} < 0$. Therefore, if $f^*_{v_t(i),i} \geq 0$, we can always find a simple path $P = [i = v_0, v_1, v_2, \ldots, v_k]$ with all flows directed from i towards v_k. Now, define $\gamma := \min(p^*_i, \min_{0\leq l\leq k-1} f^*_{v_l,v_{l+1}}, -p^*_{v_k}) > 0$. Construct a new flow $\tilde{\boldsymbol{f}}$ by uniformly decreasing by γ the flows only along the path P, i.e. $\tilde{f}_l = f^*_l - \gamma$ for $l \in P$, and $\tilde{f}_l = f^*_l$ otherwise. Define $\tilde{\boldsymbol{p}} = \boldsymbol{p}^* - \gamma \boldsymbol{e}_{i,v_k}$. The tree structure guarantees that they satisfy constraints (4c) and (4b). In addition, one can check that $\tilde{\boldsymbol{p}}$ also satisfy constraint (4d). However, the constructed flow $\tilde{\boldsymbol{f}}$ yields a strictly lower cost, contradicting the assumption that $\boldsymbol{p}^*$ is optimal. If $p^*_{u_t(i)} < \overline{p}_{u_t(i)}$, we can similarly define $\gamma := \min(p^*_i, -f^*_{u_t(i),i}, \overline{p}_{u_t(i)} - p^*_{u_t(i)}) > 0$, and let $\tilde{\boldsymbol{p}} = \boldsymbol{p}^* - \gamma \boldsymbol{e}_{i,u_t(i)}$. It can be checked that $\tilde{\boldsymbol{p}}$ is feasible and that the corresponding flow $\tilde{\boldsymbol{f}}$ achieves lower cost, contradicting the assumption that $\boldsymbol{p}^*$ is optimal. □

Proof of Lemma 4. (i) For the sake of contradiction, suppose $p^*_s \geq 0$. For every other node $i \neq s$, we have $s \in \mathcal{U}_s(i)$ and $p^*_s > \underline{p}_s$. Theorem 3 then implies that $p^*_i \geq 0$. Thus, we have $\sum_{i\in\mathcal{V}} p^*_i \geq p^*_s > 0$, which contradicts the power balancing condition. Therefore, $p^*_s \leq 0$. Similarly, we can show $p^*_t \geq 0$.

(ii) Define $\mathcal{V}_+ = \{i \in \mathcal{V} : p^*_i > 0\}$ as the set of nodes with positive injection deviations at optimum. The claim that $\sum_{i\in\mathcal{V}} |p^*_i| \leq 2\alpha$ is equivalent to $\sum_{i\in\mathcal{V}_+} p^*_i \leq \alpha$ since $\boldsymbol{p}^*$ is balanced. For the sake of contradiction, assume $\sum_{i\in\mathcal{V}_+} p^*_i > \alpha$. It is easy to check that $t \in \mathcal{V}_+$ and $s \notin \mathcal{V}_+$. Let $\hat{\boldsymbol{p}} = \boldsymbol{p}^* + \alpha \boldsymbol{e}_{s,t}$. Considering the set $\mathcal{V}_+$ as a group, the flow conservation rule implies that there exists a line $(i, j_1) \in \mathcal{E}$ with $i \in \mathcal{V}_+$, $j_1 \in \mathcal{V} \setminus \mathcal{V}_+$ and $f^*_{i,j_1} > 0$. If $p^*_{j_1} = 0$, one can further find another $j_2 \in \mathcal{V} \setminus \mathcal{V}_+$ with $(j_1, j_2) \in \mathcal{E}$ and $f^*_{j_1 j_2} > 0$. We can repeat this process and the flow conservation rule guarantees that there must exist a path $P := [i, j_1, j_2, \ldots, j_k]$ such that $p^*_i > 0$, $p^*_{j_1}, \ldots, p^*_{j_{k-1}} = 0$, and $p^*_{j_k} < 0$ with non-zero flows from node i towards node k. Similarly to the proof of Lemma 2, we can uniformly reduce the flow by $\gamma := \min(p^*_i, \min_{l\in P} f^*_l, -p^*_{j_k})$ with feasible injections $\tilde{\boldsymbol{p}} = \boldsymbol{p}^* - \gamma \boldsymbol{e}_{i,j_k}$. This leads to a strictly smaller objective, which contradicts the optimality of $\boldsymbol{p}^*$. □

Proof of Theorem 6. Along the lines of Lemma 2, we can show that if $p^*_i > 0$ and $i \neq t$, then there exists a path P connecting node t and i such that $f^*_{u^P_t(i),i} < 0$ and $p^*_{u^P_t(i)} = \overline{p}_{u^P_t(i)}$. Applying this claim repeatedly yields Theorem 6(a) and (b).

To prove such a claim, we follow a strategy similar to that of Lemma 2. Define $\hat{\boldsymbol{p}} := \boldsymbol{p}^* + \alpha \boldsymbol{e}_{s,t}$. For the sake of contradiction, assume that $f^*_{u^P_t(i),i} \geq 0$ for every path connecting t and i. Then, there must exist a simple path $P' = [i = v_0, v_1, v_2, \ldots, v_k]$ such that $t \notin P'$, $f^*_{v_l,v_{l+1}} > 0$ for $0 \leq l \leq k-1$, and $\hat{p}_{v_1} = \cdots = \hat{p}_{v_{k-1}} = 0, \hat{p}_{v_k} < 0$. Define $\gamma := \min(p^*_i, \min_{0\leq l\leq k-1} f_{v_l,v^*_{l+1}}, -p^*_{v_k}) > 0$. Construct a new power injection vector $\tilde{\boldsymbol{p}} = \boldsymbol{p}^* - \gamma \boldsymbol{e}_{i,v_k}$, which can be checked to satisfy the $\underline{\boldsymbol{p}} \leq \tilde{\boldsymbol{p}} \leq \overline{\boldsymbol{p}}$. We further have $\tilde{\boldsymbol{p}} + \alpha \boldsymbol{e}_{s,t} = C\tilde{\boldsymbol{f}}$, where $\tilde{f}_l := f^*_l - \gamma$ for $l \in P'$ and $\tilde{f}_l := f^*_l$ otherwise. Given that the corresponding flow $\boldsymbol{f}' := BC^T L^\dagger(\tilde{\boldsymbol{p}} + \alpha \boldsymbol{e}_{s,t})$ minimizes (2), we have $\boldsymbol{f}'^T B^{-1} \boldsymbol{f}' \leq \tilde{\boldsymbol{f}}^T B^{-1} \tilde{\boldsymbol{f}} < \boldsymbol{f}^{*T} B^{-1} \boldsymbol{f}^*$. Thus we have constructed a feasible $\tilde{\boldsymbol{p}}$ with a strictly lower objective, which contradicts the assumption that $\boldsymbol{p}^*$ is optimal. One can similarly prove that $p^*_{u^P_t(i)} = \overline{p}_{u^P_t(i)}$.

Finally, the last part of the theorem, which states that $f^*_{i,j} = 0$ if $\underline{p}_i < p^*_i < \overline{p}_i$ and $\underline{p}_j < p^*_j < \overline{p}_j$, can be proved from the KKT conditions of problem (4). □